

RESEARCH ARTICLE



OPEN ACCESS

Received: 02-05-2024

Accepted: 03-06-2024

Published: 25-06-2024

Citation: Ashok P, Unnisa H, Kumar RU, Reddy MCK (2024) Influence of Magneto-hydrodynamic with Williamson Nanofluid Flow Control of Forcheeimer Model under Chemical Reaction. Indian Journal of Science and Technology 17(25): 2658-2666. <https://doi.org/10.17485/IJST/v17i25.1484>

* **Corresponding author.**ashokpiitkgp@gmail.com**Funding:** None**Competing Interests:** None

Copyright: © 2024 Ashok et al. This is an open access article distributed under the terms of the [Creative Commons Attribution License](https://creativecommons.org/licenses/by/4.0/), which permits unrestricted use, distribution, and reproduction in any medium, provided the original author and source are credited.

Published By Indian Society for Education and Environment ([iSee](https://www.iseeindia.org/))

ISSN

Print: 0974-6846

Electronic: 0974-5645

Influence of Magneto-hydrodynamic with Williamson Nanofluid Flow Control of Forcheeimer Model under Chemical Reaction

Pegadapalli Ashok^{1*}, Haleem Unnisa², Rama Udai Kumar³,
M Chenna Krishna Reddy¹

¹ Department of Mathematics, University College of Sciences, Osmania University, Hyderabad, 500007, Telangana, India

² Department of Mathematics, DR.V.R.K Women's College of Engineering & Technology, Moinabad, 500075, Telangana, India

³ Department of Mathematics, Keshav Memorial College of Engineering, Ibrahimpatnam, 501510, Telangana, India

Abstract

Objective: The research focused on Williamson's nonlinear governing flow on Magneto hydrodynamic incompressible, steady fluid over a porous stretching sheet in a two-dimensional direction. The permeable stretching sheet embedded by Williamson fluid is based on the flow model of non-Darcy Forchheimer law with chemical reaction. This article concentrated on an energy equation dominated by the dissipation parameter analysis. **Methods:** The governing mathematical partial derivative formulations are changed to a system of ordinary differential formulations with appropriate similarity transformation. The mathematical formulations are evaluated employing the numerical method of the R-K fourth-order scheme. MATLAB software bvp4c is used for computing numerical results. The numerical results and graphs were successfully demonstrated with the R-K fourth-order system. **Findings:** For the influence of Williamson non-Newtonian, non-fluid observed emerging dimensionless quantifiers such as Williamson number, porous, electric, thermophoresis, Brownian motion, Prandtl, and Schmidt dimensionless number respectively. The performance of non-dimensional parameters is investigated in detail. **Novelty:** As described in the results, Williamson's non-Newtonian nanofluid under the influence of magneto-hydrodynamics is mentioned as a new value to the existing literature. The gained results are the innovative study of the influence of chemical reaction on Williamson non-Newtonian nanofluid and magnetic strength and reported on dimensionless parameters.

Keywords: Electric parameter; Williamson Nanofluid; Darcy-Forchheimer; Viscous dissipation; Chemical reaction quantifier

1 Introduction

The important role of Nano-size particles is suspended in non-Newtonian phase change which was observed by Ghalambaz⁽¹⁾. The metals, oil, ethylene, glycol, and carbides of conventional fluids of water are examples of nanoparticles. The thermal properties of base fluids are enhanced by the suspension of nanoparticles. In many engineering and research applications, the effectiveness of chemical, and nuclear reactors and the aeronautical industry depends upon energy and concentration transportation. Williamson non-Newtonian nano-fluid comprehend with MHD via hybrid nanoparticle was studied by Abdul Majeed et al.⁽²⁾. Rammanjiini et al.⁽³⁾ described an unsteady Williamson nanofluid via stretching plate for the effect of mixed convection of the Riga plate model. The research report revealed the thermal and solutal status of the inner flow region which are waning with the effect of stratification parameters.

Reshu⁽⁴⁾ has discussed micropolar fluid flow with heat and mass transfer electrically between two stretchable disks. A few researchers discussed the view of combined effects of Magneto hydro dynamic and electrical with viscous dissipation and MHD effect on stretching sheet bio-convective medium and numerical outputs are concentrated at stagnation point flow. The medical field bearings and MHD generator functions are dominated by magnetic and electric inputs. Gopal et al.⁽⁵⁾ contributed investigations on chemical reactions and Jagadha et al.⁽⁶⁾ tested nano-fluid on the different geometrical models in two as well as three-dimensional ways.

The investigation of electrically conductive MHD second-grade fluid models of MHD, water-based nanofluids peristaltic governing flow, and examined Joule heating in the mixed convective medium. Prasanna Kumar et al.⁽⁷⁾ analyzed forced and natural convection MHD Williamson nanofluid under porous media with the chemical reaction of melting and transferring heat. Srinivasacharya et al.⁽⁸⁾ performed mixed i.e., forced and natural convection with chemical processing and radiation in saturated porosity. Recently Faisal et al.⁽⁹⁾ studied about characteristics of heat and mass transfer hydro-magnetic field with the enhancement of Casson nano-fluid.

The exploration of the chemical reaction of Williamson Nano-fluid is very less. This research study is concentrated in association with the above. The entire document information is correct and not published elsewhere. Thermal radiative nanofluid in a stretching sheet obeying non-Darcy in a convection medium was discussed by Kishan et al.⁽¹⁰⁾ in the current research investigation we discussed Williamson non-Newtonian nanofluid under the influence of electrical and magnetic strength and reported on dimensionless parameters, order chemical reaction and viscous dissipation over a model of stretching sheet. The momentum and energy governing flow formulations possess nonlinear partial derivatives and electrical and magnetic range quantifiers. The sustainable method Runge-Kutta computed employing MATLAB software to output the numerical results graphically.

2 Problem Formulation

We consider Williamson's non-Newtonian two-dimensional incompressible flow for the model of stretching sheet exponentially. The stretching sheet is embedded with Williamson nanofluid, the origin of the fluid is the starting point of the sheet. The axis is directed towards the sheet and the y -axis is perpendicular to it. The velocity gradient of Williamson nanofluid at the surface of the sheet is the product of the reference velocity (U_0) and length of the sheet exponentially, i.e., the geometrical model of Williamson nanofluid is sketched in Figure 1.

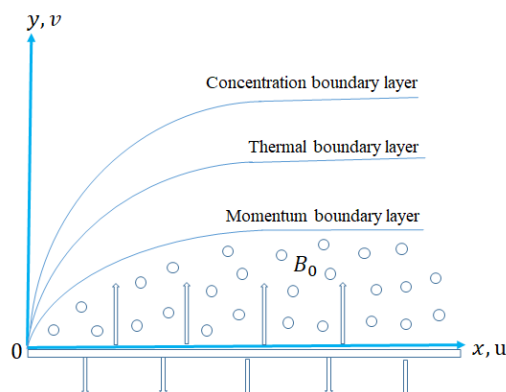


Fig 1. The Geometrical model of Williamson nanofluid flow chart

The notations of variable velocity (v_w), heat flux at sheet surface maintaining constant level, (q_w) and ambient fluid temperature are considered. The external force of magnetic strength is applied parallel to the axis. Based on the above-mentioned subject conditions including Bossiness approximations, the governing Williamson nanofluid equations⁽¹¹⁻¹⁶⁾ are framed

$$\frac{\partial u^*}{\partial x^*} + \frac{\partial v^*}{\partial y^*} = 0 \quad (1)$$

$$u^* \frac{\partial u^*}{\partial x^*} + v^* \frac{\partial u^*}{\partial y^*} = \frac{\mu}{\rho} \frac{\partial^2 u^*}{\partial y^{*2}} + \frac{C_f \sqrt{K_1}}{\nu} \frac{\partial}{\partial y} (u^2) + \sqrt{2\nu} \frac{\partial u^*}{\partial y^*} \frac{\partial^2 u^*}{\partial y^{*2}} - \frac{\sigma}{\rho} B_o^2 u^* - \frac{\nu u^*}{K_p} \quad (2)$$

$$u^* \frac{\partial T^*}{\partial x^*} + v^* \frac{\partial T^*}{\partial y^*} = \frac{k}{\rho c_p} \frac{\partial^2 T^*}{\partial y^{*2}} + \frac{\mu}{\rho c_p} \left(\frac{\partial u^*}{\partial y^*} \right)^2 + \frac{\sigma}{\rho c_p} u^* B_o^2 + \frac{(\rho c)_p}{(\rho c)_f} \left[D_B \frac{\partial C^*}{\partial y^*} \frac{\partial T^*}{\partial y^*} + \frac{D_T}{T_\infty} \left(\frac{\partial T^*}{\partial y^*} \right)^2 \right] \quad (3)$$

$$u^* \frac{\partial C^*}{\partial x^*} + v^* \frac{\partial C^*}{\partial y^*} = D_B \frac{\partial^2 C^*}{\partial y^{*2}} + \frac{D_T}{T_\infty} \frac{\partial^2 T^*}{\partial y^{*2}} - K_n^* (C^* - C_\infty^*) \quad (4)$$

The inner flow region is measured to the below-mentioned conditions:

$$u^* = U^*, v^* = -v_w^*, -k \left(\frac{\partial T^*}{\partial y^*} \right) = q_w, (C_y) = q_s \text{ at } y^* = 0$$

$$u^* \rightarrow 0, T^* \rightarrow T_\infty^*, C^* \rightarrow C_\infty^* \text{ as } y^* \rightarrow \infty \quad (5)$$

Taking v_o as constant, we assumed v_w^* as $v_o e^{\frac{x}{2L}}$

The non-dimensional quantifiers are

$$\xi = y^* \sqrt{\frac{U^*}{2\nu L}}, u^* = U^* f'(\xi), v^* = -\sqrt{\frac{\nu U^*}{2L}} (f(\xi) + \xi f'(\xi)), \theta(\xi) = \frac{k}{q_w} (T - T_\infty) \sqrt{\frac{Re}{2L^2}}$$

$$We = \sqrt{\frac{2u_o^3}{\nu}} e^{\frac{x}{2L}}, Er = \frac{E_o}{B_o u_o e^{\frac{x}{2L}}}, Ec = \frac{U^{*2} k}{C_p q_w} \sqrt{\frac{\nu Re}{2L^2}}$$

$$Ha^2 = \frac{\sigma B_o^2}{\rho u_o}, N_b = \frac{(\rho c)_p}{(\rho c)_f} \frac{D_B q^* w \sqrt{2L}}{k \nu \sqrt{U^*}}, N_t = \frac{(\rho c)_p}{(\rho c)_f} \frac{D_T q^* w \sqrt{2L}}{k T_\infty \nu \sqrt{U^*}}$$

$$\Gamma = \frac{2\delta_n (q_w^*)^{n-1} L}{U^*}, Sc = \frac{\nu}{D}, \lambda = \frac{C_f \sqrt{2K_1 Re}}{\nu} \quad (6)$$

Utilizing the physical quantifiers, the Equations are

$$f''' (1 + we f'') + 2\lambda f' f'' - \left(\frac{f'}{K_p} \right) + f f'' - 2f'^2 + Ha^2 (f') = 0 \quad (7)$$

$$\theta'' + Pr (f' \theta + \theta' f) + Pr Ec f'^2 + Pr Ha^2 Ec (f')^2 + Pr N_b \theta' \phi' + Pr N_t \theta'^2 = 0 \quad (8)$$

$$\phi'' + (f' \phi + \phi' f) Sc + \theta'' \frac{Nt}{Nb} - Sc \delta \phi = 0 \quad (9)$$

The initial and concern-subjected boundary conditions are

$$f = f_w, f' = 1, \theta' = -1, \phi = 1 \text{ at } \xi = 0$$

$$f' \rightarrow 0, \theta \rightarrow 0, \phi \rightarrow 0 \text{ as } \xi \rightarrow \infty \quad (10)$$

3 Introduction To Runge-Kutta Method

The Runge-Kutta system is extensively used and an effective system for numerally solving differential equations for the initial-value problems. Recently studied about RK-Method by Abdel Salam et al. (17–20)

Introducing special variable notations changing non-linear higher order formulations to linear differential equations.

$$f = y(1), f' = y(2), f'' = y(3), \theta = y(4), \theta' = y(5), \phi = y(6), \phi' = y(7)$$

The Equations (7), (8) and (9) are modified forms of first-order ODE.

$$y'(2) = y(3), y''(3) = (1/(1 + wey(3))) \left(\left(\frac{1}{K_p} \right) y(2) - y(1)y(3) + 2y(2)y(2) \right) - 2\lambda y(2)y(3) - Ha.Ha(y(2))$$

$$y'(4) = y(5), y'(5) = \begin{bmatrix} -Pr(y(2)y(4) + y(1)y(5)) - PrHa^2Ec(y(2))^2 \\ -PrNby(5)y(7) - PrNty(5)y(5) \end{bmatrix}$$

$$y'(6) = y(7), y'(7) = \left(-Scy(2)y(6) - Scy(7)y(1) - y'(5) \left(\frac{Nt}{Nb} \right) - Sc\delta y(6) \right)$$

The dimensionless parameters are the representations of the physical significance of the Williamson Nano-fluid governing flow, and the flow control outputs of the inner flow region are illustrated graphically employing MATLAB Software.

4 Results And Discussion

To present the impacts of all physical interpretations of dimensionless quantifiers of values are fixings $Er, Ha, K_p, Pr, Sc, Ec, \delta, \lambda, n$ on the velocity gradient, energy field, and concentration profiles. The graphs are displayed in the physical interpretations 2-11.

Figures 2, 3, 4 and 5 elucidate the impact of suction and injection on profiles of energy $\theta(\xi)$ and concentration $\phi(\xi)$ for thermophoresis parameters Nt . It is noteworthy that energy and concentration are an increasing function of thermophoresis parameter Nt subjected to both suction $f_w > 0$ and injection $f_w < 0$. Due to more heat in the energy flow region, the temperature gradient increases in both cases. It is seen that being far away from the solid body boundary layer increases concentration, as witnessed in Figures 3 and 5.

Figures 6, 7, 8 and 9 display the impact of range quantifier Brownian motion Nb subject to suction $f_w > 0$ and injection $f_w < 0$ conditions on thermophoresis and concentration quantifier. It is described that the energy flow rate declines for higher values of injection input parameters for both energy and species profiles. Figures 7 and 9 reported that boundary layer thickness is more compared to the energy equation for larger numerical inputs of the Brownian motion parameter Nb . The study of the graphical presentation shows the thermophoresis and concentration profiles have less growth for both suction $f_w > 0$ and injection $f_w < 0$. The collision of nanoparticles of Williamson nanofluid leads to a decline in energy and concentration field. The flow behavior of temperature and concentration distribution is the same as in the Williamson nanofluid governing flow.

Figure 10 illustrates that momentum is a decreasing function in the velocity profile. The behavior of Williamson nanofluid is analyzed by Weissenberg number We , and higher estimations of its inputs are plotted graphically. The impact of electric magnetic strength leads to the upsurge of the velocity gradient of Williamson nanofluid. Figure 11 revealed the effect of the permeability parameter acting as an aiding flow of Williamson nanofluid in the momentum equation. The velocity gradient enhances larger values of the permeability quantifier.

5 Conclusion

5.1 Novelty, Prospectus, and Recommendation

The main objectives of this article are mathematically defined as Williamson non-Newtonian nano-fluid flow under the influence of chemical and magnetic strength and reported on dimensionless parameters order of chemical reaction and viscous dissipation over a model of stretching sheet. The numerical values are found using shooting techniques.

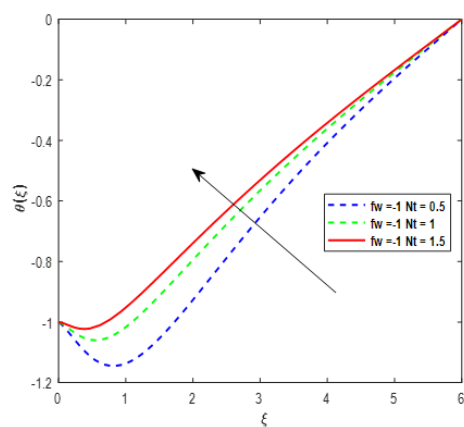


Fig 2. Graphical output of Nt

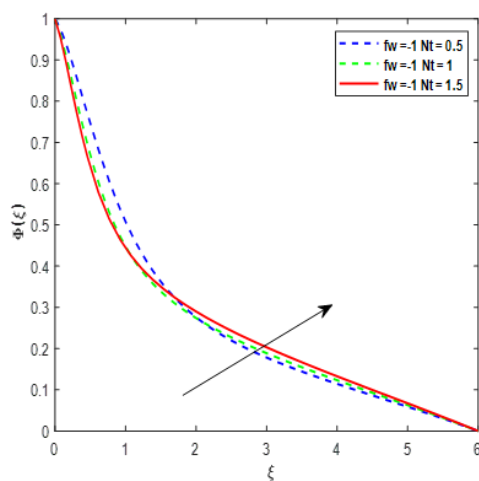


Fig 3. Graphical output of Nt

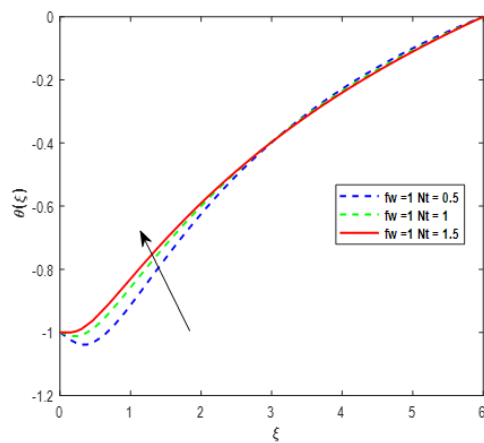


Fig 4. Graphical output of Nt

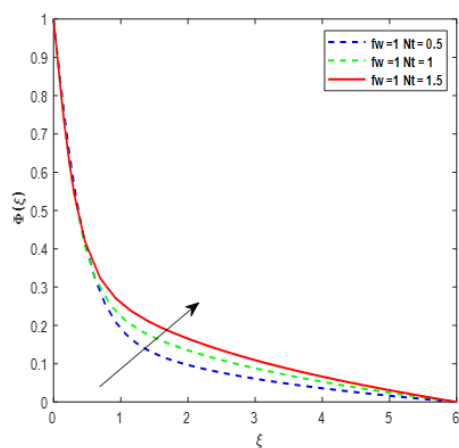


Fig 5. Graphical output of Nt

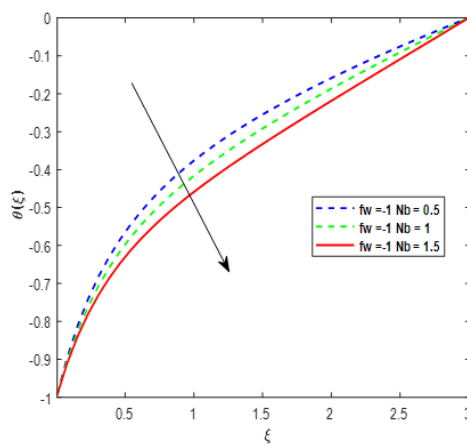


Fig 6. Graphical output of Nb

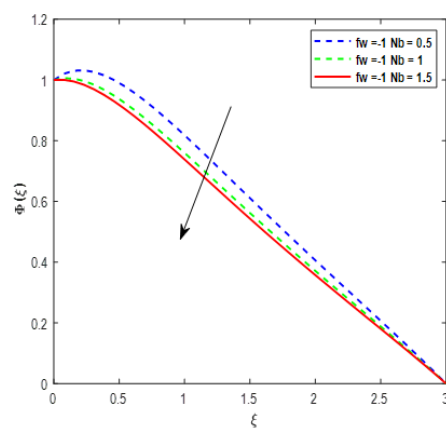


Fig 7. Graphical output of Nb

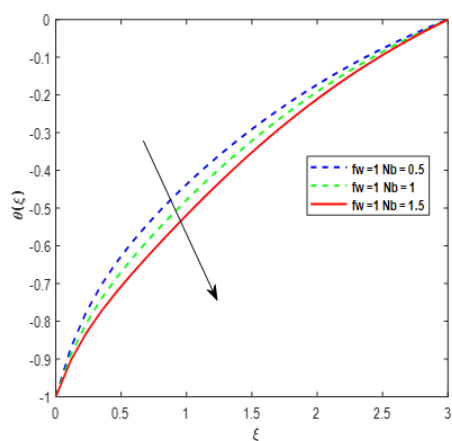


Fig 8. Graphical output of Nb

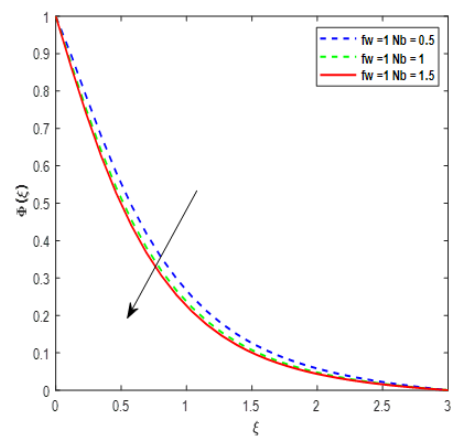


Fig 9. Graphical output of Nb

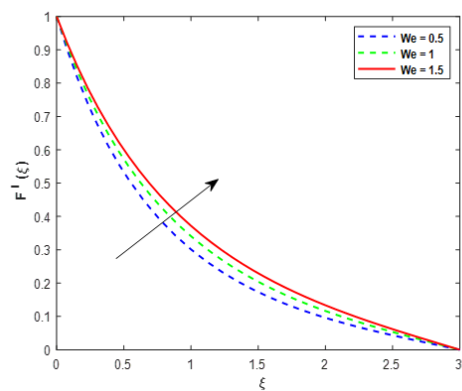


Fig 10. Graphical output of We

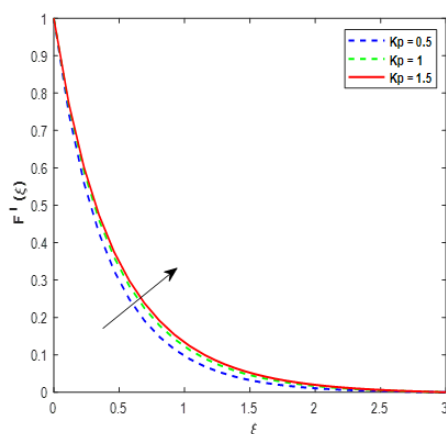


Fig 11. Graphical output of K_p

5.2 Importance of work

This paper clarifies the 2-dimensional Forcheeimer model of magneto-hydrodynamics. Williamson Nanofluid stretching surface entrenched by Weissenberg number Nano-scale seized particles, incompressible laminar flow subjected to steady condition. The governing parameters are viscous dissipation, chemical reaction parameter, and chemical reaction quantifier are graphically clarified.

- The energy level gradient enhances for thermophoresis parameter, viscous dissipation, and Prandtl except Brownian parameter.
- The enhancement in species gradient for higher inputs of thermophoresis, order of chemical reaction, Prandtl and magnetic except chemical reaction quantifier, Brownian motion parameter, and Schmidt quantifier.
- The injection and suction effect is more in thermophoresis, order of chemical reaction, and viscous dissipation. The increment of movement of injection is observed in Brownian motion, magnetic, and viscous dissipation.

References

- 1) Ghalambaz M, Mehryan SAM, Tahmasebi A, Hajjar A. Non-Newtonian phase-change heat transfer of nano-enhanced octadecane with mesoporous silica particles in a tilted enclosure using a deformed mesh technique. *Applied Mathematical Modelling*. 2020;85:318–337. Available from: <https://doi.org/10.1016/j.apm.2020.03.046>.
- 2) Almanee A. Numerical study on heat and mass transport enhancement in MHD Williamson fluid via hybrid nanoparticles. *Alexandria Engineering Journal*. 2022;61(10):8343–8354. Available from: <https://doi.org/10.1016/j.aej.2022.01.041>.
- 3) Ramanjini V, Krishna GG, Mishra SR, Sailajakumari SV, Sree HK. An unsteady axisymmetric Williamson nanofluid flow over a radially stretching Riga plate for the inclusion of mixed convection and thermal radiation. *Partial Differential Equations in Applied Mathematics*. 2022;6:1–13. Available from: <https://doi.org/10.1016/j.padi.2022.100456>.
- 4) Agarwal R. Heat and mass transfer in electrically conducting micropolar fluid flow between two stretchable disks. *Materials Today: Proceedings*. 2021;46(Part 20):10227–10238. Available from: <https://doi.org/10.1016/j.matpr.2020.11.614>.
- 5) Gopal D, Saleem S, Jagadha S, Ahmad F, Almatroud AO, Kishan N. Numerical analysis of higher chemical reaction on electrically MHD nanofluid under influence of viscous dissipation. *Alexandria Engineering Journal*. 2021;60(1):1861–1871. Available from: <https://doi.org/10.1016/j.aej.2020.11.034>.
- 6) Jagadha S, Gopal D, Kumar PV, Kishan N, Durgaprasad P. Three dimensional MHD nanofluid stagnation point flow with higher order chemical reaction. *Journal of Thermal Engineering*. 2022;8(2):286–298. Available from: <https://doi.org/10.18186/thermal.1086264>.
- 7) Krishnamurthy MR, Prasannakumara BC, Gireesha BJ, Gorla RSR. Effect of chemical reaction on MHD boundary layer flow and melting heat transfer of Williamson nanofluid in porous medium. *Engineering Science and Technology, an International Journal*. 2016;19(1):53–61. Available from: <https://doi.org/10.1016/j.jestch.2015.06.010>.
- 8) Srinivasacharya D, Reddy GS. Chemical reaction and radiation effects on mixed convection heat and mass transfer over a vertical plate in power-law fluid and saturated porous medium. *Journal of the Egyptian Mathematical Society*. 2016;24(1):108–115. Available from: <https://doi.org/10.1016/j.joems.2014.10.001>.
- 9) Duraihem FZ, Devi RLVR, Prakash P, Sreelakshmi TK, Saleem S, Durgaprasad P, et al. Enhanced heat and mass transfer characteristics of multiple slips on hydro-magnetic dissipative Casson fluid over a curved stretching surface. *International Journal of Modern Physics B*. 2023;37(23). Available from: <https://doi.org/10.1142/S0217979223502296>.
- 10) Reddy CS, Naikoti K, Rashidi MM. MHD flow and heat transfer characteristics of Williamson nanofluid over a stretching sheet with variable thickness and variable thermal conductivity. *Transactions of A Razmadze Mathematical Institute*. 2017;171(2):195–211. Available from: <https://doi.org/10.1016/j.trmi.2017.02.004>.

- 11) Lone SA, Ali F, Saeed A, Bognár G. Irreversibility analysis with hybrid cross nanofluid of stagnation point and radiative flow (TiO₂+CuO) based on engine oil past a stretchable sheet. *Heliyon*. 2023;9(4):1–20. Available from: <https://doi.org/10.1016/j.heliyon.2023.e15056>.
- 12) Shah SAA, Awan AU. Significance of magnetized Darcy-Forchheimer stratified rotating Williamson hybrid nanofluid flow: A case of 3D sheet. *International Communications in Heat and Mass Transfer*. 2022;136. Available from: <https://doi.org/10.1016/j.icheatmasstransfer.2022.106214>.
- 13) Hayat T, Kiyani MZ, Alsaedi A, Khan MI, Ahmad I. Mixed convective three-dimensional flow of Williamson nanofluid subject to chemical reaction. *International Journal of Heat and Mass Transfer*. 2018;127(Part A):422–429. Available from: <https://doi.org/10.1016/j.ijheatmasstransfer.2018.06.124>.
- 14) Thumma T, Mishra SR, Abbas A, Bhatti M, Sara MM, Abdelsalam I. Three-dimensional nanofluid stirring with non-uniform heat source/sink through an elongated sheet. *Applied Mathematics and Computation*. 2022;421. Available from: <https://doi.org/10.1016/j.amc.2022.126927>.
- 15) Ramesh K, Jagadha S, Gopal D, Naik SHS, Kishan N. One dimensional radiative nanofluid flow with heat generative Al₂ O₃-H₂O and Cu-H₂O nanoparticles reactions chemically. In: 2ND INTERNATIONAL CONFERENCE & EXPOSITION ON MECHANICAL, MATERIAL, AND MANUFACTURING TECHNOLOGY (ICE3MT 2022). AIP Conference Proceedings. . Available from: <https://doi.org/10.1063/5.0190329>.
- 16) Madhu M, Shashikumar NS, Thriveni K, Gireesha BJ, Mahanthesh B. Irreversibility analysis of the MHD Williamson fluid flow through a microchannel with thermal radiation Irreversibility analysis of the MHD Williamson fluid flow through a microchannel with thermal radiation. *Waves in Random and Complex Media*. 2022. Available from: <https://doi.org/10.1080/17455030.2022.2111473>.
- 17) Abdelsalam SI, Zaher AZ. Biomimetic amelioration of zirconium nanoparticles on a rigid substrate over viscous slime - a physiological approach. *Applied Mathematics and Mechanics*. 2023;44:1563–1576. Available from: <https://doi.org/10.1007/s10483-023-3030-7>.
- 18) Abdelsalam SI, Alsharif AM, Elmaboud YA, Abdellateef AI. Assorted kerosene-based nanofluid across a dual-zone vertical annulus with electroosmosis. *Heliyon*. 2023;9(5):1–15. Available from: <https://doi.org/10.1016/j.heliyon.2023.e15916>.
- 19) Abdelsalam SI, Bhatti MM. Unraveling the nature of nano-diamonds and silica in a catheterized tapered artery: highlights into hydrophilic traits. *Scientific Reports* . 2023;13:1–17. Available from: <https://doi.org/10.1038/s41598-023-32604-6>.
- 20) Abdelsalam SI, Magesh A, Tamizharasi P, Zaher AZ. Versatile response of a Sutterby nanofluid under activation energy: hyperthermia therapy. *International Journal of Numerical Methods for Heat & Fluid Flow*. 2024;34(2):408–428. Available from: <https://doi.org/10.1108/HFF-04-2023-0173>.